BRIEF ARTICLE **Open Access**

Biomechanical assessment of a professional road cyclist following recovery from severe injury: A case report

Jonathan Sinclair[1]✉, Graham Theobald[2], Steve Atkins[1], Sian P Weeks[1], Howard T Hurst[1]

Abstract

The incidence of injury in top level road cyclists is relatively high. In a recent longitudinal study over four years using a cohort of elite road cyclists it was documented that only 15.6 % remained injury free. Acute fracture injuries accounted for 48.5 % of the total number of injuries with 26.5 % of these acute injuries being sustained in the lower extremities. This case report refers to an elite level, professional, road cyclist who returned to competition following severe fractures to the left femur and right ankle, sustained during a serious road traffic accident. The athlete reported power imbalances and feeling of dysfunction upon their return to competition. Bilateral 3-D kinematics and EMG analyses of the lower extremities were obtained. Clear asymmetries were observed in a number of 3-D kinematic parameters. These suggest an overreliance on coronal and transverse plane motions to compensate for reductions in sagittal plane movement as a result of the injury. Such outcomes have both clinical and performance implications which are discussed fully. This innovative use of advanced 3-D kinematic analysis in conjunction with isokinetic and electromyographic techniques shows the value of sports science support in improving long term performance outcomes, following a significant period of rehabilitation.

Keywords: 3-D kinematics, EMG, isokinetic dynamometer, injury, recovery

✉ **Contact email:** *jsinclair1@uclan.ac.uk* (J. Sinclair)

[1] Division of Sport, Exercise and Nutritional Sciences, University of Central Lancashire, United Kingdom

[2] Allied Health, University of Central Lancashire. The Body Rehab: Injury and Rehabilitation Clinic, Kendal, United Kingdom

Received: 11 July 2012. Accepted: 28 January 2013.

Introduction

The incidence of injury in top level road cyclists is relatively high (Barrios et al. 1997 and Bohlmann 1981). In a recent longitudinal study over four years using a cohort of elite road cyclists it was documented that only 15.6 % remained injury free (Bernardo et al. 2012). Acute/traumatic injuries accounted for 48.5 % of the total number of injuries with 26.0 % of these acute injuries being sustained in the lower extremities (Bernardo et al. 2012).

In the present study a case report of an elite road cyclist who has returned from a severe injury is presented. The participant was involved in a road accident with an articulated vehicle and suffered severe fractures to the left femur and right ankle. The injuries sustained required the insertion of surgical pins to both right and left sides. The right side was subsequently removed following sufficient recovery but metalwork securing the left femur remains in place. The injury required 6 months of recovery before returning to training and competition. To our knowledge, this case study is the first to utilise advanced 3-D kinematic analysis to assess performance function in cycling, following a serious injury.

Although the associated injuries have now healed and the cyclist has been cleared medically to return to elite level competition several complications have emerged following recovery. Firstly the participant has reported decreased capacity to maintain power output during longer races >100km. Secondly the cyclist has reported low back pain and left hip discomfort during both daily activities and professional cycling. This has been attributed to power imbalances and feeling of dysfunction following the accident. Therefore, whilst it must be acknowledged that the cyclist is still competitive at elite level, the participant has indicated that their performance is diminished directly due to the injuries sustained in the accident.

The aim of the current case report is to examine the 3-D kinematics, isokinetic and electromyographic (EMG) parameters of the cyclist in order to determine whether any biomechanical asymmetries exist. Key outcomes will be considered with regard to the influence on performance, and provide insight into the aetiology of lower back pain.

Materials and methods

Participants

A single male participant (Age 25 years, Mass 74 kg, height 1.74 m) was examined. The participant was a professional cyclist, who had been a national champion in both road and time trial events. The participant completed a health screen questionnaire and written

informed consent was obtained in accordance with the declaration of Helsinki. Ethical approval was obtained from the university ethical committee for postgraduate research.

in each condition 200W, 400W, and 600W. Power output was determined using a professional model SRm powermeter (SRm, Jülich, Germany) attached to the participants own cycle mounted on a CycleOps fluid 2 indoor trainer (Saris, Colorado, USA). Data were collected for 20 s during each trial and a total of five trials were obtained. A total of five pedal cycles from each limb were extracted from each trial. Cadence and gear choice were self-selected to achieve the required power output. All kinematic data were captured at 250Hz via an eight camera motion analysis system (Qualisys Medical, Goteburg, Sweden). Calibration of the QualysisTM system was performed before data collection. Only calibrations which produced average residuals of less than 0.85 mm for each camera for a 750.5mm wand length and points above 4000 in all cameras were accepted prior to data collection.

The marker set used for the study was based on the CAST technique (Cappozo et al. 1995). The anatomical reference frames of the pelvis, left and right thigh, left and right shank and left and right foot segments were defined using retro-reflective markers attached to the 1st and 5th metatarsal heads, medial and lateral malleoli, medial and lateral epicondyle of the femur, iliac crest, anterior superior iliac spines (ASIS) and posterior superior iliac spines (PSIS). Hip joint centre was determined based on the Bell, et al. (1989) equations via the positions of the PSIS and ASIS markers. Tracking clusters were positioned on the shank and thigh. Each rigid cluster comprised four 19mm spherical reflective markers mounted to a thin sheath of lightweight carbon fibre with length to width ratios of 2.05-1 and 1.5-1 for the femur and tibia respectively, in accordance with the Cappozzo et al. (1997) recommendations. A static trial was conducted with the participant in the anatomical position allowing the positions of the anatomical markers to be referenced in relation to the tracking clusters, following which they were removed.

EMG

Surface EMG activity was obtained synchronously with 3-D kinematics, at 1000 Hz, from the left and right Vastus Lateralis (VL), Vastus Medialis (VM), Gastrocnemius (GM) and Rectus Femoris (RF) muscles, at 1000 Hz. Biometrics bipolar electrodes (model SX230) (Biometrics Ltd., UK) with an inter-electrode distance of 20 mm were utilized. All electrodes were placed in alignment with the muscle pennation on the bellies on the muscles in accordance with the SENIAM guidelines (Freriks et al. 1999). The skin was shaved and abraded with abrasive paper and cleaned with ethanol wipes to reduce the amount of skin impedance. The electrodes and electrode wires were wrapped on thigh and shank with an elastic bandage, to prevent dislocation.

Procedure

3-D kinematics

The participant completed five trials

Isokinetics

An ISOCOM® dynamometer (Eurokinetics Limited, UK) was used to measure bilateral joint torque of the ankle (plantar and dorsi flexors), knee (flexors and extensors), and hip (flexors and extensors) throughout the available active range of motion. The appropriate limb was positioned with the anatomical axis of rotation of the appropriate joint aligned with the axis of rotation of the lever arm of the dynamometer. Restraining straps were placed around the shoulders, chest and waist, with an additional restraint applied to the thigh (proximal to the knee joint), in order to stabilize body segments and prevent any extraneous body movement. All joint motions were conducted at an angular velocity of 60 °.sec-1. Contraction type was concentric in flexion and extension with a 1 s rest period between repetitions. Three maximal efforts from all three joints were performed for each movement, and peak power and peak torque were extracted.

Data Processing

All data were normalized to 100% of the pedal cycle for both right and left limbs. Trials were processed in Qualisys Track Manager in order to identify anatomical and tracking markers then exported as C3D files. Kinematic parameters were quantified using Visual 3-D (C-Motion, Germantown, USA) after marker data were smoothed using a low-pass (Butterworth 4th order zero-lag filter) at a cut off frequency of 15Hz. This cut-off frequency was determined from identifying the frequency where 95% of the signal content was maintained. 3-D kinematics of the hip, knee and ankle joints were calculated using an XYZ cardan sequence of rotations where X = sagittal; Y = coronal plane and Z = transverse plane rotations (Sinclair et al. 2012a). In addition to this 3-D movements of the pelvis segment were reported relative to the lab co-ordinate system. 3-D kinematic measures from the hip, knee, ankle and pelvis which were extracted for statistical analysis were 1) angle at top dead centre 1 (TDC1), 2) angle at top dead centre 2 (TDC2), 3) range of motion during the pedal cycle (ROM), 4) peak angle during the pedal cycle and 5) relative range of motion from TDC1 to peak angle.

The EMG signals from each muscle were full wave rectified and filtered using a 20 Hz Butterworth zero lag low-pass 4th filter to create a linear envelope. EMG data from each muscle were normalised using the peak pedal cycle EMG amplitude obtained at 600 W from an ensemble average of the three completed trials (Sinclair et al. 2012b). EMG measures extracted were; the mean normalized amplitude during the pedal cycle (% NORM).

Statistical Analyses

Descriptive statistics (means and standard deviations) were calculated for the outcome measures using SPSS 19.0 (SPSS Inc, Chicago, USA).

Results

The data indicates some notable bilateral imbalances in 3-D kinematics across a range of power outputs (Table 1-4 & Figure 1-2). In addition bilateral imbalances were also observed in muscle recruitment magnitude and also isokinetic peak force development (Table 4-5 & Figure 3). These findings may point towards reduced bilateral function.

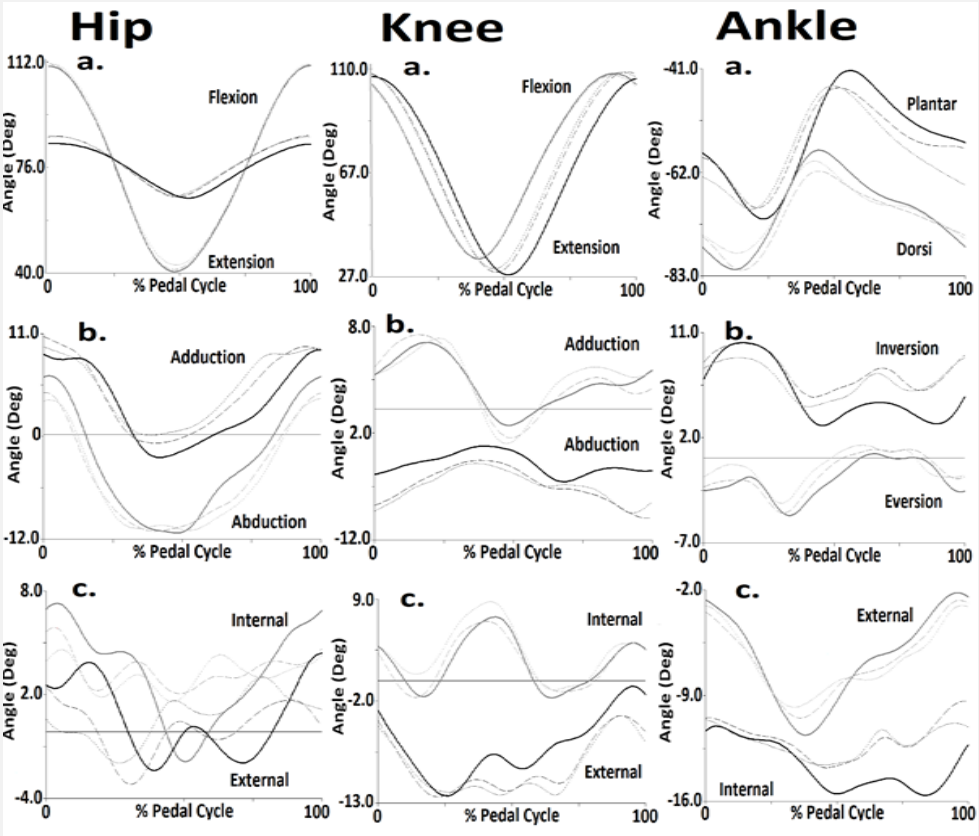

Figure 1. Hip, knee and ankle joint kinematics in the a. sagittal, b. coronal and c. transverse planes (Black = right limb & Grey = left limb) Solid line = 600, Dashed line = 400 and Dotted line = 200W.

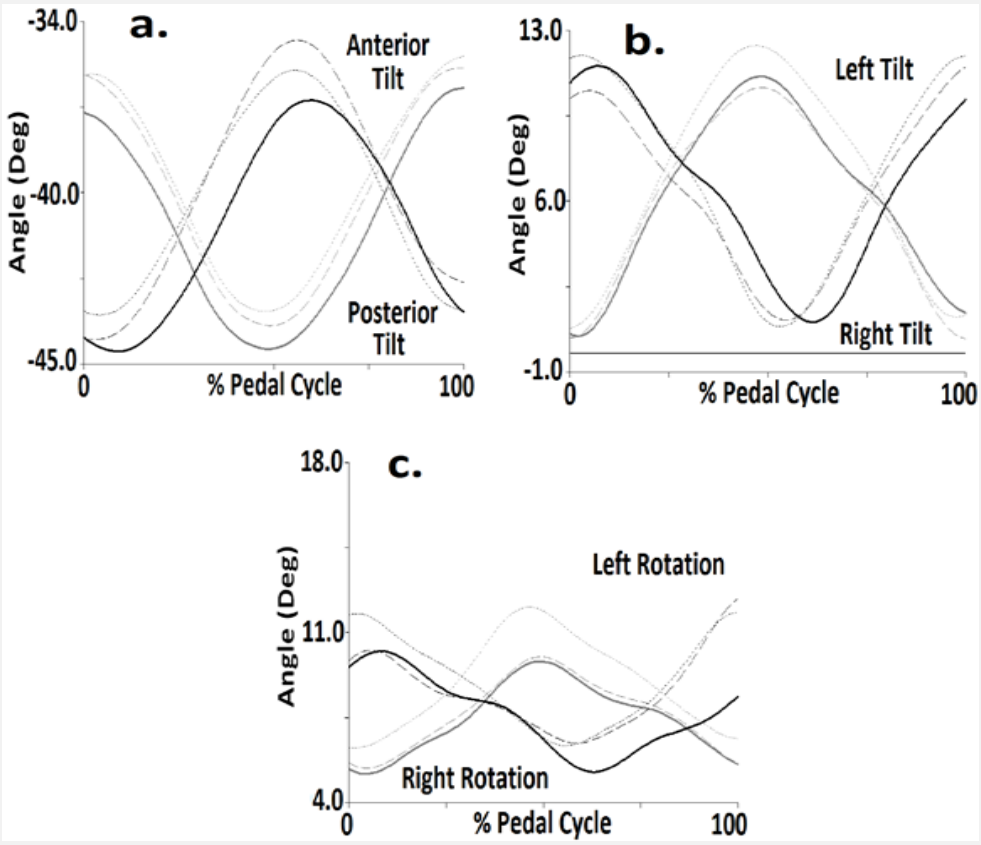

Figure 2. Hip, knee and ankle joint kinematics at 600W in the a. sagittal, b. coronal and c. transverse planes (Black = right limb & Grey = left limb), Solid line = 600, Dashed line = 400 and Dotted line = 200W.

Table 1. Hip, Knee and ankle joint kinematics (means and standard deviations) from the right and left limbs at 600W.

	Hip			Knee			Ankle		
Sagittal Plane (+ =flexion/ - =extension)	**Right**	**Left**	**Mean Difference**	**Right**	**Left**	**Mean Difference**	**Right**	**Left**	**Mean Difference**
TDC1 (°)	84.18 ± 0.14	110.19 ± 0.27	26.01	104.67 ± 0.19	101.64 ± 0.30	3.03	-58.11 ± 1.03	-77.31 ± 0.99	19.20
TDC2 (°)	83.90 ± 0.40	110.48 ± 0.012	26.58	103.89 ± 0.43	101.56 ± 0.46	2.33	-55.96 ± 0.28	-77.22 ± 0.75	21.26
Peak Angle (°)	65.55 ± 0.17	40.70 ± 0.45	24.85	27.25 ± 0.55	33.63 ± 1.15	6.40	-41.16 ± 0.23	-57.49 ± 1.26	16.33
ROM (°)	0.28 ± 0.40	0.29 ± 0.18	0.01	0.78 ± 0.29	0.18 ± 0.04	0.60	2.15 ± 1.18	0.20 ± 0.21	1.95
Relative ROM (°)	18.63 ± 0.06	69.43 ± 0.62	50.80	77.42 ± 0.44	68.02 ± 1.42	9.40	16.95 ± 1.09	19.82 ± 1.63	2.87
Coronal plane (+ =adduction/ =abduction)									
TDC1 (°)	-5.89 ± 0.76	3.13 ± 0.16	9.02	9.00 ± 0.39	6.47 ± 0.41	2.53	6.92 ± 0.32	-2.83 ± 0.64	9.75
TDC2 (°)	-5.56 ± 1.38	3.54 ± 0.24	9.10	9.51 ± 0.70	6.50 ± 0.34	3.01	5.36 ± 1.02	-2.91 ± 0.52	8.27
Peak Angle (°)	-6.60 ± 0.31	-6.06 ± 0.27	0.54	-2.55 ± 0.15	-9.66 ± 0.49	7.11	2.64 ± 0.77	-0.77 ± 0.84	3.44
ROM (°)	0.91 ± 1.86	0.41 ± 0.24	0.50	0.57 ± 0.48	0.08 ± 0.04	0.49	1.55 ± 1.12	0.13 ± 0.05	1.42
Relative ROM (°)	0.71 ± 0.46	9.22 ± 0.73	8.51	11.56 ± 0.45	12.19 ± 0.69	0.63	4.28 ± 0.89	2.07 ± 1.47	2.21
Transverse plane (+ =internal/ - =external)									
TDC1 (°)	2.71 ± 0.64	7.11 ± 0.63	4.40	-3.15 ± 0.90	3.63 ± 0.07	6.78	-10.90 ± 0.37	-2.03 ± 0.08	8.87
TDC2 (°)	4.55 ± 0.24	6.98 ± 0.30	2.43	-1.49 ± 2.48	3.25 ± 0.36	4.74	-11.84 ± 0.51	-1.83 ± 0.15	10.01
Peak Angle (°)	4.64 ± 0.18	1.73 ± 0.76	2.91	-3.36 ± 1.38	6.31 ± 0.98	9.67	-15.40 ± 0.23	1.54 ± 0.17	16.94
ROM (°)	1.84 ± 0.47	0.51 ± 0.07	1.33	3.03 ± 0.97	0.38 ± 0.33	2.65	0.93 ± 0.28	0.21 ± 0.10	0.72
Relative ROM (°)	1.93 ± 0.54	5.84 ± 0.65	3.91	2.78 ± 2.33	3.00 ± 1.91	0.22	4.49 ± 0.33	3.60 ± 0.21	0.89

Table 2. Hip, Knee and ankle joint kinematics (means and standard deviations) from the right and left limbs at 400W.

	Hip			Knee			Ankle		
Sagittal Plane (+ =flexion/ - =extension)	**Right**	**Left**	**Mean Difference**	**Right**	**Left**	**Mean Difference**	**Right**	**Left**	**Mean Difference**
TDC1 (°)	86.66 ± 0.38	110.96 ± 0.36	24.30	105.79 ± 0.68	100.93 ± 0.61	4.86	-59.03 ± 0.61	-75.13 ± 1.23	16.10
TDC2 (°)	86.80 ± 0.81	110.87 ± 0.74	24.07	105.52 ± 0.92	101.58 ± 1.18	3.94	-57.21 ± 2.63	-74.93 ± 1.64	17.72
Peak Angle (°)	66.93 ± 0.04	41.43 ± 0.40	25.50	28.23 ± 0.41	33.65 ± 1.20	5.42	-44.80 ± 1.60	-61.78 ± 1.52	16.98
ROM (°)	0.55 ± 0.50	0.36 ± 0.06	0.19	0.51 ± 0.58	0.98 ± 1.28	0.47	1.93 ± 2.13	1.23 ± 0.83	0.70
Relative ROM (°)	20.73 ± 0.35	69.53 ± 0.43	48.78	77.51 ± 0.27	67.28 ± 1.50	10.23	14.27 ± 2.02	13.35 ± 2.09	0.92
Coronal plane (+ =adduction/ =abduction)									
TDC1 (°)	-8.66 ± 0.68	3.84 ± 0.27	12.50	10.96 ± 0.36	4.72 ± 0.49	6.24	8.39 ± 0.59	-2.51 ± 0.39	10.90
TDC2 (°)	-9.81 ± 1.75	1.88 ± 2.09	11.69	9.50 ± 0.45	4.68 ± 0.52	4.82	9.03 ± 0.70	-1.68 ± 2.50	10.71
Peak Angle (°)	-9.87 ± 1.69	-6.76 ± 0.66	3.11	-1.05 ± 0.56	-9.82 ± 0.47	8.77	5.33 ± 1.00	-1.12 ± 0.55	6.45
ROM (°)	1.15 ± 1.08	2.23 ± 1.88	1.08	1.46 ± 0.42	0.18 ± 0.10	1.28	0.86 ± 0.83	1.46 ± 1.74	0.60
Relative ROM (°)	1.21 ± 1.02	9.91 ± 0.84	8.70	12.01 ± 0.37	9.12 ± 0.85	2.89	3.06 ± 1.29	1.40 ± 0.90	1.66
Transverse plane (+ =internal/ - =external)									
TDC1 (°)	2.62 ± 1.01	5.78 ± 0.43	3.16	-4.24 ± 1.09	2.88 ± 0.70	7.12	-10.04 ± 0.61	-2.00 ± 0.27	8.04
TDC2 (°)	0.33 ± 3.24	4.79 ± 0.73	4.46	-5.43 ± 1.93	3.38 ± 1.09	8.81	-8.93 ± 1.83	-1.98 ± 0.32	6.95
Peak Angle (°)	2.67 ± 1.17	-1.99 ± 0.36	4.66	-2.94 ± 0.90	5.29 ± 0.97	8.23	-13.48 ± 0.34	1.88 ± 0.29	15.36
ROM (°)	2.29 ± 2.23	0.99 ± 0.85	1.30	1.70 ± 1.87	0.52 ± 0.47	1.18	1.11 ± 1.22	0.17 ± 0.05	0.94
Relative ROM (°)	0.14 ± 0.24	7.89 ± 0.91	7.75	1.30 ± 1.21	2.57 ± 0.30	1.27	3.43 ± 0.41	4.91 ± 0.20	1.48

Table 3. Hip, Knee and ankle joint kinematics (means and standard deviations) from the right and left limbs at 200W.

	Hip		Mean Difference	Knee		Mean Difference	Ankle		Mean Difference
Sagittal Plane (+ =flexion/ - =extension)	**Right**	**Left**		**Right**	**Left**		**Right**	**Left**	
TDC1 (°)	86.21 ± 0.55	110.98 ± 0.53	24.77	105.55 ± 0.85	101.62 ± 0.88	3.93	-62.99 ± 0.75	-74.75 ± 0.82	11.76
TDC2 (°)	86.36 ± 0.21	110.99 ± 0.52	24.63	104.24 ± 1.84	100.57 ± 0.43	3.67	-64.64 ± 2.34	-75.60 ± 0.82	10.96
Peak Angle (°)	66.47 ± 0.37	42.98 ± 0.34	23.49	29.68 ± 0.53	34.19 ± 0.49	4.51	-44.28 ± 1.64	-59.71 ± 1.11	15.43
ROM (°)	0.31 ± 0.06	0.41 ± 0.31	0.10	1.88 ± 1.97	1.19 ± 1.11	0.69	1.65 ± 2.06	0.85 ± 0.45	0.80
Relative ROM (°)	19.74 ± 0.91	68.00 ± 0.19	48.26	75.89 ± 0.33	61.43 ± 0.50	14.46	18.71 ± 1.16	15.04 ± 0.52	3.67
Coronal plane (+ =adduction/ =abduction)									
TDC1 (°)	-9.18 ± 0.51	3.14 ± 0.88	12.32	9.84 ± 0.48	3.78 ± 0.41	6.06	7.78 ± 0.02	-1.63 ± 0.69	9.41
TDC2 (°)	-8.39 ± 0.69	3.35 ± 0.44	11.74	9.67 ± 0.99	4.07 ± 0.63	5.60	8.80 ± 0.87	-1.49 ± 0.39	10.29
Peak Angle (°)	-9.62 ± 0.50	-6.47 ± 0.39	3.15	-0.08 ± 0.45	-9.35 ± 0.44	9.27	4.49 ± 0.50	-1.51 ± 0.66	2.98
ROM (°)	0.89 ± 0.70	0.49 ± 0.51	0.40	0.90 ± 0.81	0.77 ± 0.45	0.13	0.91 ± 0.85	0.42 ± 0.38	0.49
Relative ROM (°)	0.45 ± 0.37	9.51 ± 1.04	9.06	9.93 ± 0.87	13.13 ± 1.41	3.20	3.40 ± 0.48	0.79 ± 0.76	2.61
Transverse plane (+ =internal/ - =external)									
TDC1 (°)	0.72 ± 0.86	4.10 ± 1.10	3.38	-4.80 ± 0.13	3.63 ± 0.97	8.60	-10.12 ± 0.56	-2.46 ± 0.05	7.66
TDC2 (°)	1.29 ± 0.91	4.40 ± 0.29	3.11	-6.53 ± 1.58	3.34 ± 0.77	9.87	-10.65 ± 0.63	-2.51 ± 0.21	8.14
Peak Angle (°)	3.19 ± 0.72	-1.60 ± 1.00	4.79	-3.58 ± 0.85	5.99 ± 0.89	9.57	-13.24 ± 0.28	2.34 ± 0.15	15.58
ROM (°)	1.09 ± 0.32	1.12 ± 0.17	0.03	1.73 ± 1.67	0.91 ± 0.31	0.82	0.53 ± 0.56	0.21 ± 0.08	0.32
Relative ROM (°)	2.47 ± 1.53	5.50 ± 0.94	3.03	1.22 ± 0.94	1.62 ± 0.85	0.40	3.12 ± 0.29	4.80 ± 0.11	1.68

Table 4. Pelvic kinematics (means and standard deviations) from the right and left limbs at 600, 400 and 200W.

	600W		400W		200W	
Anterior / Posterior tilt (+ =anterior/ - =posterior)	**Right**	**Left**	**Right**	**Left**	**Right**	**Left**
TDC1 (°)	-44.26 ± 0.51	-36.10 ± 0.60	-44.16 ± 0.48	-35.89 ± 0.55	-43.12 ± 0.55	-35.78 ± 0.50
TDC2 (°)	-43.20 ± 0.42	-35.65 ± 0.54	-42.86 ± 0.39	-35.40 ± 0.48	-42.86 ± 0.40	-35.39 ± 0.46
Peak Angle (°)	-37.50 ± 0.36	-44.14 ± 0.39	-35.34 ± 0.20	-43.70 ± 0.30	-36.39 ± 0.29	-43.10 ± 0.34
ROM (°)	1.24 ± 0.11	0.43 ± 0.14	2.68 ± 0.13	0.49 ± 0.09	0.36 ± 0.24	0.28 ± 0.10
Relative ROM (°)	7.05 ± 0.40	8.10 ± 0.51	8.88 ± 0.32	7.85 ± 0.46	7.10 ± 0.35	7.20 ± 0.38
Left / Right tilt (+ =left/ =right)						
TDC1 (°)	11.48 ± 0.61	0.85 ± 0.40	0.83 ± 0.37	1.06 ± 0.42	12.01 ± 0.36	1.01 ± 0.46
TDC2 (°)	10.22 ± 0.40	1.10 ± 0.29	11.28 ± 0.39	1.06 ± 0.42	12.24 ± 0.32	0.96 ± 0.39
Peak Angle (°)	1.76 ± 0.20	10.20 ± 0.36	2.25 ± 0.28	9.94 ± 0.30	2.02 ± 0.39	12.38 ± 0.60
ROM (°)	1.20 ± 0.10	0.24 ± 0.09	0.37 ± 0.12	0.23 ± 0.10	0.21 ± 0.12	0.05 ± 0.10
Relative ROM (°)	9.60 ± 0.24	9.40 ± 0.30	8.61 ± 0.20	9.10 ± 0.48	9.97 ± 0.39	11.36 ± 0.40
Left / Right rotation (+ =left/ - =right)						
TDC1 (°)	9.69 ± 0.68	5.02 ± 0.28	9.81 ± 0.51	5.32 ± 0.35	11.89 ± 0.52	6.15 ± 0.37
TDC2 (°)	8.10 ± 0.49	5.44 ± 0.30	12.71 ± 0.30	5.39 ± 0.40	12.60 ± 0.39	6.10 ± 0.35
Peak Angle (°)	5.26 ± 0.20	9.03 ± 0.42	6.88 ± 0.38	9.20 ± 0.50	6.75 ± 0.80	12.62 ± 0.30
ROM (°)	1.56 ± 0.20	0.40 ± 0.16	2.90 ± 0.13	0.06 ± 0.08	0.70 ± 0.12	0.05 ± 0.06
Relative ROM (°)	4.40 ± 0.46	4.00 ± 0.40	2.91 ± 0.48	3.88 ± 0.42	5.12 ± 0.43	6.45 ± 0.33

Discussion

The aim of the current case report was to examine the 3-D kinematics, isokinetic and electromyographic (EMG) parameters of an elite cyclist who has returned to competition following a severe trauma. This case report represents to our knowledge the first to document the resultant biomechanical and neuromuscular profile following an injury of this nature.

The results indicate that the cyclist exhibits a number of asymmetrical imbalances. At the hip joint, the left limb is associated with sizeable increases in both TDC angle and relative range of motion in comparison to the right side. The values obtained for the left side are considerably greater than those documented by Umberger and Martin, (2001) and Gregor and Conconi (2000). This was evident at all levels of power output. It is hypothesized that this is attributable to a lack of torque and power production, and serves as an adaptive mechanism as a result of the injury. Hip extension, to bottom dead centre, has been linked strongly to the transfer of power to the pedals during cycling (Elmer et al. 2011).

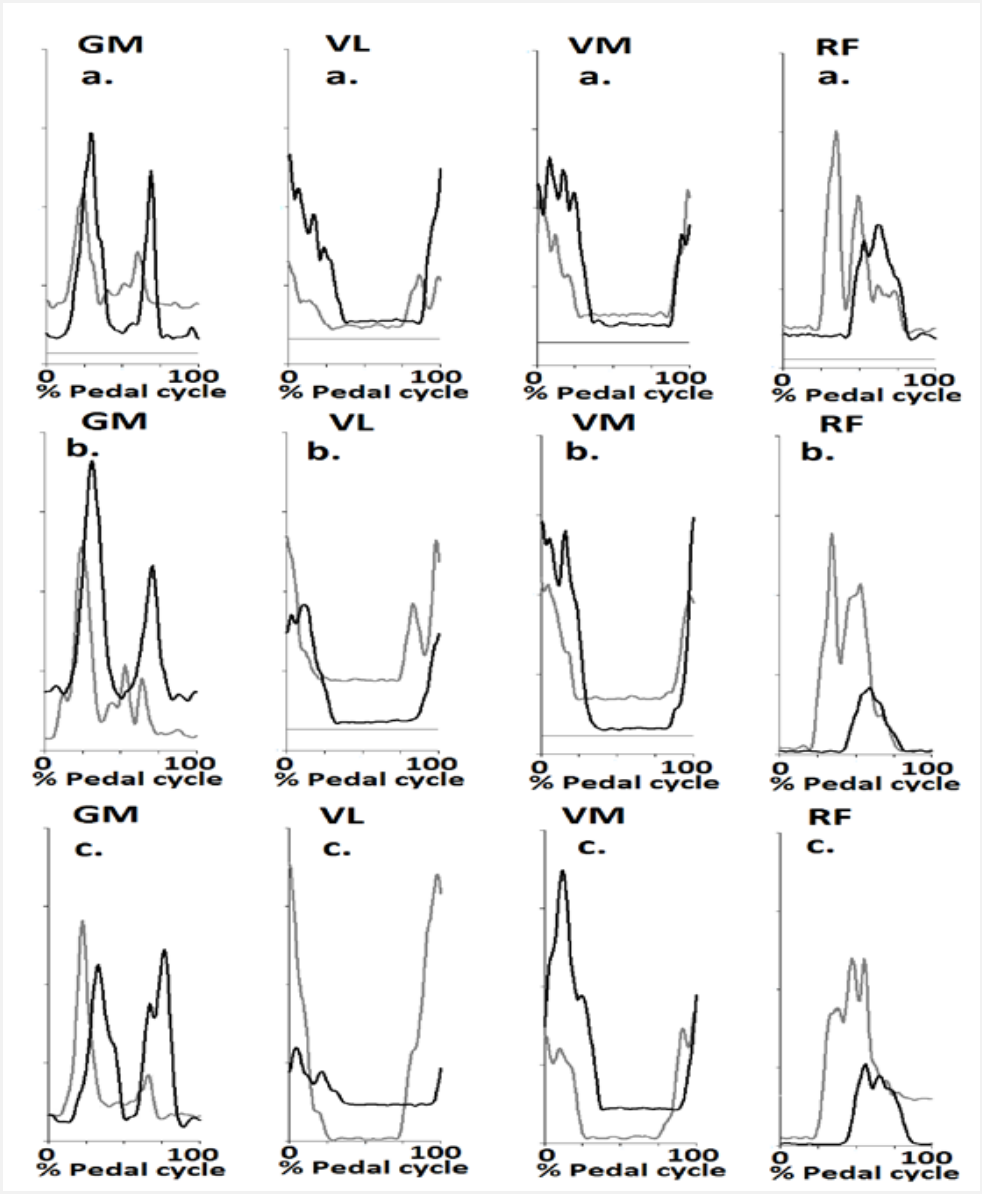

Figure 3. EMG patterns from the GM, VL, VM and RF a. 600, b. 200 and c. 600 W (Black = right limb & Grey = left limb).

In addition, the left hip was also associated with increases in both coronal and transverse plane relative ranges of motion. This may relate to the reduction in power production in the left limb which may require additional contributions from outside the sagittal plane in an attempt to maintain balance. The values extracted from the analysis of pelvic kinematics provide further support for this notion. As the upper left musculature was found to be comparatively weaker than the right, it is likely that the left side generates extra force from muscle groups and stabilizers supporting the pelvis. This may be the reason that the left pelvis is tilted to the left for the entire pedal cycle. This may also have clinical implications for the development of lower back pain reported by the participant. The continual leftwards tilting of the pelvis, due to increases in sagittal plane relative range of motion, in conjunction with increases in adduction and internal rotation ranges of motion may facilitate the development of lower back pathology.

Table 5. Normalized EMG amplitudes (means and standard deviations) from the right and left limbs.

	600 W		400 W		200 W	
	Right	Left	Right	Left	Right	Left
GM (% NORM)	0.29 ± 0.03	0.19 ± 0.02	0.24 ± 0.05	0.13 ± 0.02	0.13 ± 0.009	0.11 ± 0.09
VL (% NORM)	0.44 ± 0.27	0.21 ± 0.007	0.19 ± 0.04	0.13 ± 0.09	0.15 ± 0.04	0.12 ± 0.008
VM (% NORM)	0.30 ± 0.06	0.23 ± 0.02	0.19 ± 0.006	0.18 ± 0.14	0.12 ± 0.04	0.11 ± 0.08
RF (% NORM)	0.26 ± 0.02	0.33 ± 0.06	0.16 ± 0.02	0.23 ± 0.03	0.13 ± 0.05	0.19 ± 0.01

Table 6. Isokinetic torque and power parameters (means) from the right and left limbs.

		Torque (Nm)		Power (W)	
		Right	**Left**	**Right**	**Left**
Hip	*Flexion*	167.8	127.8	132.0	111.9
	Extension	161.1	116	109.6	91.6
Knee	*Flexion*	106.6	103.3	91.8	86.5
	Extension	220.5	167.1	180.0	133.9
Ankle	*Plantar*	57.6	75.2	169.2	459.6
	Dorsi	21.5	23.6	16.9	26.2

At the knee joint the left limb was associated with reductions in sagittal plane relative range of motion in comparison to the right. This is consistent with the reductions in isokinetic extension power and torque, and may relate to the injury sustained to the left femur. This may be a compensatory mechanism in relation to the large increases in hip relative range of motion. This bilateral difference was not as pronounced as at the hip joint and the values quoted remained similar to those extracted by Umberger and Martin, (2001) and Gregor and Conconi (2000). In addition, the left knee is also associated with increases in coronal plane abduction when compared to the right. This has potential performance implications as increases in knee abduction have been shown to reduce the extent to which the rider can apply force to the pedals (Bini et al. 2009).

At the ankle joint, although the sagittal plane waveforms were qualitatively similar the right limb was associated with greater plantar flexion throughout the pedal cycle across all power outputs. The right ankle angulation in the sagittal plane differed in magnitude from the values documented by Umberger and Martin, (2001) who found that the ankle was less dorsiflexed throughout the pedal cycle. The right ankle was also associated with sizeable reductions in peak isokinetic plantar flexion torque and power output. It is likely that this relates to dysfunction due to the injury sustained to the right ankle whereby the cyclist is unable to achieve the same levels of dorsiflexion in comparison to the left.

The EMG analyses revealed that, in general, the right side was associated with greater muscular recruitment across all power outputs when compared to the left. This is consistent with the kinematic and isokinetic observations, and is likely to be a compensatory mechanism for the lack of power delivery from the left side. Of particular interest is the double firing rate in the right GM in comparison to the left. This again may relate to a lack of power in the left side, whereby in addition to contraction at 90°, to the GM also contracts on the upstroke at 270° around to stiffen the ankle joint and assist in hip musculature and aid right side hip musculature pull the crank around to compensate the potentially reduced force application of the left limb. This may also relate to the injury sustained to the right ankle joint whereby the observed firing patterns of the GM serve as a protective mechanism to avoid any further discomfort/ injury to the affected area.

Considering the consistent and considerable decrease in power of the left side musculature, it is likely that early onset fatigue is understandable and expected. Cycling is reliant on bilateral balance in power output and stability across the joints and musculature (Carpes et al. 2010). Imbalance of this nature means that the right side fatigues earlier than normal and there is resultant compensation. During longer races in excess of 200km it is inconceivable that the right side can compensate fully for these dysfunctions. It should be re-stated that the cyclist is still able to compete at the highest level, but it is highly likely that this injury is currently having a negative influence on his career although the extent to which performance is affected is difficult to determine.

In conclusion whilst the cyclist has returned to function and been medically cleared to resume competition following surgery and rehabilitation, the questions as to whether sport specific function has been restored, and whether every day and sport specific function are distinct remains. It is likely, and recommended, that the cyclist will require considerable rehabilitation on the areas outlined in these analyses to return to pre-accident levels of cycling performance. Based on the observations of the current investigation it is recommended that the cyclist seek to re-establish bilateral symmetry and range of motion across all lower extremity joints and musculature. This will involve strengthening exercises applied to the left limb hip flexors (illipsoas, rectus femoris, and psoas major) and extensors (gluteus maximus and hamstrings). It is also advocated that strengthening exercises should be

undertaken for the right side ankle plantar (gastrocnemius, soleus and tibialis posterior) and dorsi flexors (tibialis anterior). In addition, given that the core musculature provides the foundation from which pedal force is generated and serves to maintain the neutral pelvic position on the bike (Mellion, 1994). It is therefore recommended that the cyclist also incorporate core training exercises into his training regimen. It is likely that this will need to be undertaken after the associated metalwork is removed as this may well be inhibiting performance further. Once the rehabilitation is complete the best way forward would be to re-test using the same protocol in order to determine the degree of recovery.

References

1. Barrios C, Sala D, Terrados N, Valenti JR, (1997). Traumatic and overuse injuries in elite professional cyclists. Sports Exercise and Injury, 3: 176–179
2. Bernardo N, Barrios C, Vera P, Laíz C, Hadala M (2012). Incidence and risk for traumatic and overuse injuries in top-level road cyclists. Journal of Sports Sciences, 30: 1047-1053
3. Bohlmann JT, (1981). Injuries in competitive cycling. Physician Sports medicine, 9: 117–126
4. Bell AL, Brand RA, Pedersen, DR, (1989). Prediction of hip joint centre location from external landmarks, Human Movement Science, 8: 3-16
5. Bini RR, Diefenthaeler FC, Felipe P, Mota CB, (2007). External work bilateral symmetry during incremental cycling exercise In: 25th International Symposium on Biomechanics in Sports, 2007, Ouro Preto - MG. v.1 .168 – 171
6. Cappozzo A, Catani F, Leardini A, Benedeti MG, Della CU, (1995). Position and orientation in space of bones during movement: Anatomical frame definition and determination, Clinical Biomechanics, 10: 171-178
7. Cappozzo A, Cappello A, Croce U, Pensalfini F, (1997). Surface-marker cluster design criteria for 3-D bone movement reconstruction. IEEE Transactions on Biomedical Engineering, 44: 1165-1174
8. Carpes FP, Mota CB, Faria IE. (2010). On the bilateral asymmetry during running and cycling - a review considering leg preference. Physical Therapy in Sport, 11: 136-142
9. Elmer SJ, Barratt PR, Korff T, Martin JC, (2011). Joint-specific power production during submaximal and maximal cycling. Medicine and Science in Sports and Exercise, 43: 1940-1947
10. Freriks B, Hermens H, Disselhorst-Klug C, Rau G, (1999). The recommendations for sensors and sensor placement procedures for surface electromyography. In: Hermens H.J, Ed. European recommendations for surface electromyography. Enschede: Roessingh Research and Development, 1999: 15-53
11. Gregor, R. J. and Conconi, F. (2000). Road Cycling: Olympic Handbook of Sports Medicine Blackwell Science Ltd. London
12. Mellion, M.B, (1994). Neck and back pain in bicycling. Clinics in Sports Medicine, 13: 137–164
13. Sinclair J, Taylor PJ, Edmundson CJ, Brooks D, Hobbs SJ, (2012a). Influence of the helical and six available cardan sequences on 3-D ankle joint kinematic parameters. Sports Biomechanics, 11: 430-437
14. Sinclair J, Brooks, D, Edmundson CJ, Hobbs SJ, (2012b). The efficacy of EMG MVC normalization techniques for running analyses. Journal of Biomechanics, 41: 621-662
15. Umberger BR, Martin PE, (2001). Testing the planar assumption during ergometer cycling, Journal of Applied Biomechanics, 17: 55-62